Volume 13 Number 2 February 2020 Pages 321-650

Energy & Environmental Science

rsc.li/ees



ISSN 1754-5706



COMMUNICATION

Energy & Environmental Science



COMMUNICATION



Cite this: Energy Environ. Sci., 2020.13.495

Received 9th August 2019, Accepted 5th November 2019

DOI: 10.1039/c9ee02571e

rsc.li/ees

Electrical decoupling of microbial electrochemical reactions enables spontaneous H2 evolution†

Xi Chen, Da Fernanda Leite Lobo, Yanhong Bian, Lu Lu, Da Xiaowen Chen, C Melvin P. Tucker, Vuxi Wang and Zhiyong Jason Ren ** **and Zhiyong Jason Ren **p***

Hydrogen evolution is not a spontaneous reaction, so current electrochemical H₂ systems either require an external power supply or use complex photocathodes. We present in this study that by using electrical decoupling, H2 can be produced spontaneously from wastewater. A power management system (PMS) circuit was deployed to decouple bioanode organic oxidation from abiotic cathode proton reduction in the same electrolyte. The special PMS consisted of a boost converter and an electromagnetic transformer, which harvested energy from the anode followed by voltage magnification from 0.35 V to 2.2-2.5 V, enabling in situ H₂ evolution for over 96 h without consuming any external energy. This proof-of-concept demonstrated a cathode faradaic efficiency of 91.3% and a maximum overall H2 conversion efficiency of 28.9%. This approach allows true self-sustaining wastewater to H₂ evolution, and the system performance can be improved via the PMS and reactor optimization.

Introduction

Hydrogen is a desired fuel and medium for fuel cell vehicles and large scale energy storage solutions, and it is an essential chemical building block for industries that produce fertilizers, polymers, plastics, pharmaceuticals, and many critical products. 1-4 Plus, hydrogen provides a complementary alternative to renewable electricity, and it can be produced using renewables such as solar and wind via water splitting or biomass and wastewater via fermentation and microbial electrolysis.5-8

Traditional water splitting requires a theoretical 1.23 V to overcome the thermodynamic barrier $(H_2O \rightarrow H_2 + 0.5O_2)$

Broader context

H₂ complements renewable electricity as a renewable fuel carrier and chemical building block, but H2 evolution is an endothermic reaction that requires external energy input to close the thermodynamic gap of water splitting. This study demonstrated unassisted H2 evolution by using an electrical decoupling strategy with a tailored power management system (PMS), which can overcome the thermodynamic gap and achieve uphill reactions by electrically decoupling the reactions and temporarily storing and transferring the energy generated from anodic organic oxidization reactions. This approach enables spontaneous H2 generation from wastewater and advances a new H2 economy.

 $\Delta G^0 = 237.2 \text{ kJ mol}^{-1}$), and in reality 1.8–2.0 V is used to overcome the potential losses associated with internal resistance, the junction potential, and the overpotential on the electrode surface.^{9,10} Electrochemical H₂ production therefore has always relied on an external bias that requires energy input and additional infrastructure. This is true even for sustainable H₂ production from renewable sources, such as artificial photosynthesis (APS), which utilizes solar energy to substitute part of the electricity input, 11,12 as well as microbial electrolysis cells (MEC), which employ a variety of organic matter as the electron donor to reduce the external voltage demand. 7,13,14 Direct photoelectrolysis of water at the interface of a semiconductor and electrolyte has been a popular APS pathway, but an external bias is still needed because most semiconductors, such as Si, InP, and GaAs, do not produce sufficient voltage to drive water-splitting due to the larger junction gap of 1.6 to 2.3 eV.15-18 This external bias can be greatly reduced when the anodic water oxidation is replaced by microbial organic oxidization, because bacteria utilizes the chemical energy embedded in organics to compensate the energy required for anode oxidation, and as a result the thermodynamic driving force required for H₂ production dramatically reduced from 1.23 V (water oxidation) to 0.12 V (acetate oxidation). 18,19 Additionally, as a variety of organics, even wastewater, can be oxidized by microbial metabolism, people attempted to approach the goal of a sustainable fuel supply based on the enormous and readily available waste streams produced in

^a Department of Civil and Environmental Engineering and Andlinger Center for Energy and the Environment, Princeton University, Princeton, NJ 08544, USA. E-mail: zjren@princeton.edu

^b Departamento de Engenharia Hidráulica e Ambiental, Universidade Federal do Ceará, Brazil

^c National Bioenergy Center, National Renewable Energy Laboratory, 15013 Denver West Parkway, Golden, USA

^d The Earth Institute and School of International and Public Affairs, Columbia University, New York, NY 10027, USA

[†] Electronic supplementary information (ESI) available: 1 video. See DOI: 10.1039/c9ee02571e

human society.²⁰ However, the aforementioned H₂ production from wastewater still relied on additional power such as electricity or solar, which is not a true waste-to-hydrogen situation. In previous work by Suraniti et al., an enzymatic biofuel cell was coupled with water electrolysis to achieve H₂ production in a glucose medium.²¹ An electrical booster and an electromagnetic transformer were included in the external circuit to condition the voltage produced by the biofuel cell and drive water electrolysis. The study demonstrated that electric circuits could help overcome the thermodynamic gap and achieve uphill reactions, though the system was only operated for 200 min.²¹ There has been no study that achieved spontaneous H₂ evolution from wastewater without any external energy input.

Considering the limited and intermittent nature of the power supply from renewable sources, a new strategy that decouples the two half electrochemical reactions in an electrolyzer was recently proposed by inserting a reversible redox mediator into the electrolyzer. The hydrogen evolution reaction (HER) on the cathode and oxygen evolution reaction (OER) on the anode were not directly coupled but rather mediated by the reversible reactions of a mediator, so the HER and OER could be decoupled and occur at different specific production rates. 4,22,23 Several mediators such as polyoxometalate phosphomolybdic acid, V³⁺, and nickel (oxy)hydroxides have been demonstrated to be capable of decoupling the electrochemical reactions of water splitting. 22,24,25 The concept of decoupling was originally proposed to separate the OER and HER in order to prevent the crossover of produced O2 and H₂, but we hypothesize here that the different reaction rates on the anode and cathode enabled by the decoupling strategy may open up opportunities for in situ energy storage and utilization. The reactions being decoupled don't have to be the OER and HER but could be any redox pair in an electrochemical cell.

In this study, we demonstrate the proof-of-concept that spontaneous H2 evolution could be achieved from wastewater by using a tailored power management system (PMS) to decouple the electrochemical reactions with O2 as a redox mediator. Since the electrochemical reactions occurred in one common electrolyte, water splitting won't be able to occur spontaneously due to the aforementioned thermodynamic barrier, but this barrier can be overcome by electrically decoupling the reactions and temporarily storing the energy generated from anodic organic oxidization reactions in the PMS. During this time, the PMS raised the voltage output high enough to enable spontaneous H2 evolution on the cathode. No external energy (even sunlight) was applied to the system, but rather the H₂ evolution was solely driven by the PMS, which accumulated energy from the anodic bio-oxidation of the wastewater, making the overall process spontaneous and exothermic. In addition, we characterized the mechanisms of the decoupling strategy, PMS design, reactor performance, and the energy flow.

Results and discussion

Principle of the electrical decoupling that enabled spontaneous H₂ evolution

Decoupling strategies are used to do more with less, and a free pulley example is used here to explain the decoupled electrochemical reactions that enabled endothermic H2 evolution

without an external power supply. Fig. 1A shows that when a balloon is directly connected to a basket, a higher lifting force is required to lift the load. This is similar to a conventional electrochemical cell, which requires a high enough external voltage to overcome the thermodynamic barrier of H₂ evolution. Fig. 1A shows a traditional microbial electrolysis cell (MEC), where the theoretical cell electromotive force $(E_{\rm emf}(V))$ is -0.12 V (-0.41 to (-0.29 V)), indicating that a > 0.12 V external bias is needed to overcome the thermodynamic barrier for H₂ production. In reality, the external voltage used was 0.6-1.2 V due to the overpotential and other losses.7,8,13

In contrast, Fig. 1B shows that when a free pulley is used, a much smaller effort is needed to lift the same load. This is analogous to the principle used in this study, where the O2 mediator and a power management system (PMS) served as an "electric pulley" to decouple the anodic and cathodic reactions and transform the driving force. By inserting a pair of O2 reduction (blue) and oxidation (pink) electrodes into the reactor, the bioanode organic oxidation was decoupled from the cathode proton reduction, and the PMS then enables temporary storage of the electrical energy harvested in the organic oxidization-O₂ reduction reaction, which was termed as the "energy generation part", and raised the output potential to realize the spontaneous "H₂ evolution part", which was the newly formed H₂O oxidization-proton reduction reaction. The PMS had dual functions: magnifying the output voltage of the energy generation part, and transferring the harvested energy electromagnetically, thus achieving DC isolation between the two pairs of electrodes. This is significant because without the electrical decoupling using the PMS, the two electrochemical reactions in one common electrolyte cannot occur separately due to their intrinsic electric connection via the solution.

The PMS primarily consisted of an energy harvesting circuit and an electromagnetic transformer placed on a specially designed flyback converter. 21,26 The energy harvesting circuit can harvest the energy generated from the bioanode, generally at the maximum power point, 27 so there is enough potential to power the whole PMS without the need for any external energy. The flyback converter is a key component that allows DC isolation that electrically decouples the chemical reactions. In the control experiment using just the energy harvesting circuit to connect the external circuit of the two reactions, a stable output voltage was achieved from the energy generation part but no current was detected in the H₂ evolution part. Without DC isolation, all the chemical oxidation and reduction reactions are connected in the electrolyte as well as through the circuit to a same electrical reference, making the whole system short circuited. The primary and secondary windings of the electromagnetic transformer are not electrically connected, so the circuits of the energy generation part and the H₂ evolution part are DC isolated, which enables two different electrical references: anode oxidation (GND1) and cathode reduction (GND2) as shown in Fig. 2A, hence avoiding the short circuit between the PMS input and output. The input energy from the energy generation part is periodically transferred from the first winding to the second winding of the transformer, and

Energy & Environmental Science

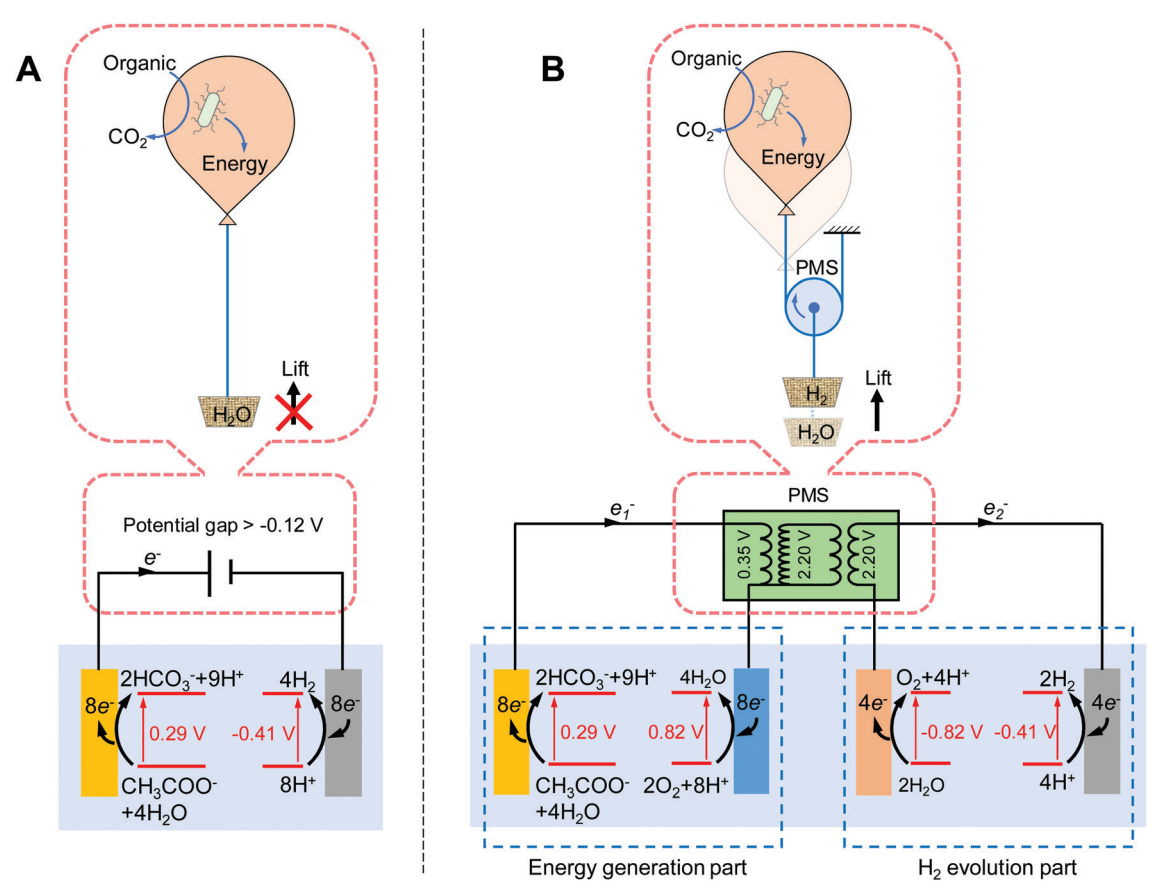


Fig. 1 Schematic of the traditional electricity-driven microbial electrolysis H_2 evolution (A) and new spontaneous H_2 evolution enabled by using tailored PMS to decouple the electrochemical reactions (B). The balloon represents the lifting force and the basket represents the objective mass to be lifted. PMS: power management system.

therefore the flyback converter is operated in a charge–discharge cycle to power H_2 generation. ^{27,28}

The input and output of the decoupling circuit

The flyback converter's capabilities of DC isolation and energy transfer were presented via a voltage input and output measured by an oscilloscope (Fig. 2B and C). Fig. 2B presents the output voltage from the energy harvesting circuit with pulse-frequency modulation (PFM) control by using a constant duty cycle and variable frequency, which is a modulation technique used in low power energy harvesters. The same voltage profile was also the flyback converter's voltage input, which was boosted to 2.16 V with a considerable ripple caused by the production of gas bubbles on the cathode surface. The boosted voltage varied according to the setting of the energy harvesting circuit control and the performance of the energy generation part. This boosted voltage was able to power the flyback and at the same time be isolated to further support H2 evolution. Fig. 2C shows a fairly constant voltage that represents the flyback converter's output voltage. This voltage (2.32 V) is similar to the flyback input voltage (2.16 V), because the flyback converter's function in this study is DC isolation and electromagnetic energy transfer. The output voltage was kept stable at around 2.3 V with a different electrical reference from the energy generation part (Fig. 2C). The voltage sign is measured to power the water splitting for H_2 production.

The PFM control used in the circuit design in this study could keep the output voltage of the energy generation part at a stable 0.35 V level, which ensures a stable input for the H₂ evolution part and leads to a 2.3 V output throughout the operation cycle. As a result, H₂ could be continuously generated until the complete consumption of the organic substrates. This demonstrates the stability and practicability of this system. Without such PFM control, the energy generation part would output a decreasing voltage over time. The input voltage of the H2 evolution part, which was boosted at a fixed magnification, would decrease correspondingly and soon result in the interruption of H₂ production when the transferred voltage could no longer support water splitting. Considering the unlimited wastewater supply in an actual situation, this system would be able to achieve long-term spontaneous H2 production. When the wastewater was replaced every 4 days to ensure a stable supply of substrates, multiple cycles of operation without an external energy supply were achieved without apparent performance decay (ESI,† Fig. S1).

Performance of the system

Each test of the system was performed in synthetic wastewater (an acetate medium) for 96 hours, and a stable electric output

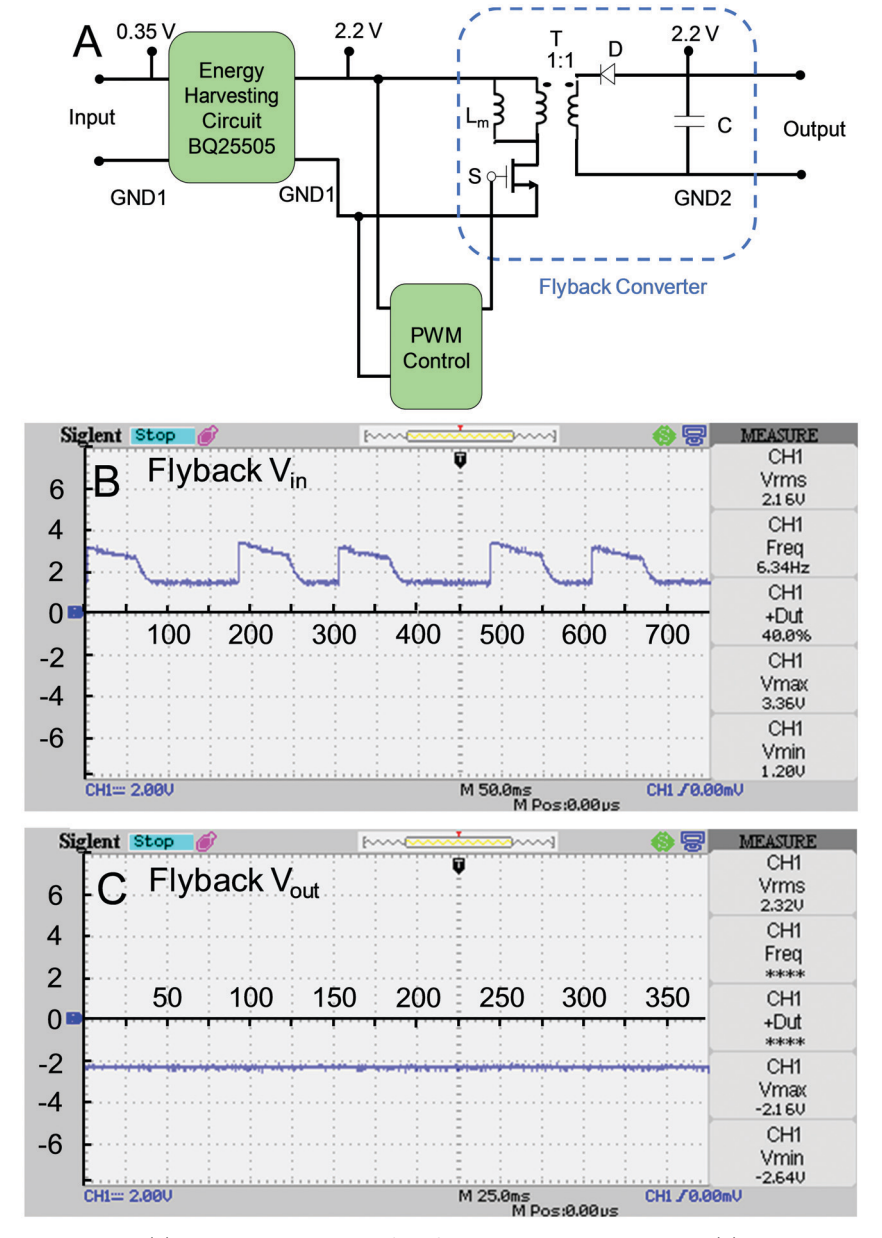


Fig. 2 Power management system design (A) and the testing results of the flyback converter input voltage (B) and output voltage (C). The output voltage from the energy harvesting circuit was also the flyback converter input voltage, which was controlled by pulse-frequency modulation using a constant duty cycle and variable frequency. PWM: pulse width modulation. (B) and (C) are real-time screen shots of the oscilloscope when testing the input and output voltage of the flyback converter, where V_{rms} (rms = root mean square) represents the effective voltage value, and +Dut represents the positive curve duty cycle.

and H_2 generation were observed (Fig. 3). Fig. 3A shows that H_2 bubbles were continuously produced from the cathode at a high rate without any external energy input (see the video clip in the ESI†). Stable H_2 generation was observed during the experiment, credited to stable current input for H_2 evolution (Fig. 3B). The time-course output voltage of the energy generation part was kept consistent at the maximum power point of 0.35 V by the PFM control circuit, while a 2.2–2.5 V voltage output was obtained from the PMS and applied to the H_2 evolution part (Fig. 3C). This *in situ* conversion of voltage enabled spontaneous H_2 evolution without external assistance.

Because of the voltage magnification, the current reduced from 2.0–2.8 mA in the energy generation part to less than 0.1 mA in the H₂ evolution part, conforming to the principle of total energy conservation (Fig. 3D). Considering the degradation of the organic substance at the anode, the conductivity of the medium decreased from 12.84 to 9.86 mS cm⁻¹, which led to an increase of the internal resistance between the anode and cathode of the energy harvesting part, thus the current output gradually decreased along the cycle. Accordingly, the current profiles of the input to the hydrogen evolution part and output from the energy generation part were analogous in shape

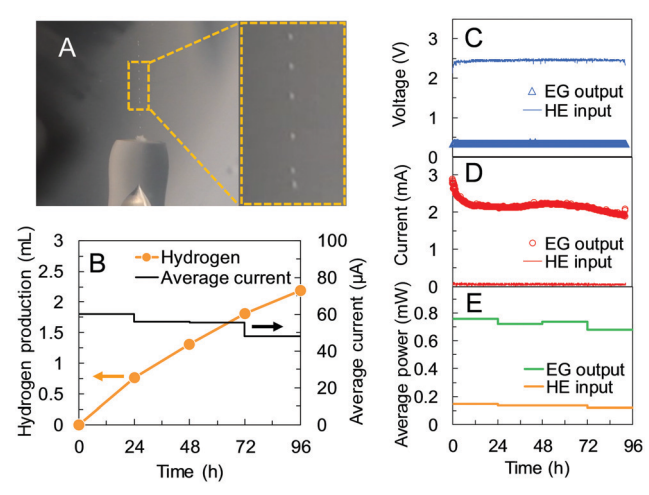


Fig. 3 Photo showing that H₂ bubbles were continuously generated on the cathode without external energy input (A); hydrogen production and average current in the hydrogen evolution circuit (B); time-course voltage (C), current (D), and average power (E) of the energy generation part output (EG output) and H₂ evolution part input (HE input).

(Fig. 3D). To avoid the interference of the ripples in the data, average powers during each 24 h were used to show the power output/input of the energy generation/H2 evolution parts, respectively (Fig. 3E). The power generation from organic degradation in the anode ranged from 0.67 to 0.95 mW during the operation, which averaged at 0.76, 0.72, 0.74, and 0.68 mW within each day, respectively. From such an energy input, average outputs of 0.15, 0.14, 0.14, and 0.12 mW were used for water splitting via the PMS magnification and transformation during the same operation period (Fig. 3E). Over 90% of the acetate in the anode was removed, representing satisfactory treatment of wastewater. The corresponding Coulombic efficiency was 34.2%. The spontaneous H2 production rate was $2.75 \text{ mL L}^{-1} \text{ day}^{-1}$, and the yield was $0.034 \text{ mol H}_2/\text{mol acetate}$. This is lower than the reported abiotic or microbial electrolysis process (which could range from 10¹ to 10⁵ mL L⁻¹ day⁻¹) due to the absence of external voltage application, 5-8 but comparable to previous reports that used enzymes to generate H2 from glucose (0.051 mol H₂/mol glucose).²¹ Based on the total coulomb input into the H₂ evolution circuit, a theoretical H₂ production rate of 3.05 mL L⁻¹ day⁻¹ could be obtained per operation cycle, representing a corresponding faradaic efficiency of 91.3%. To further improve the H₂ production performance, the O₂ evolution anode may be replaced by a bioanode to reduce the thermodynamic gap of the H₂ evolution part. In this way, a lower input voltage and a larger current would be realized to produce H2 at higher rates and efficiencies. The main advantages of this study however come from the low operational cost, zero energy input, and long sustainability with concurrent benefits of wastewater treatment.

System efficiency and energy analysis

Fig. 4 shows the energy efficiency and energy flow of the system. During a typical 96 h operation, an average 0.73 mW of power was generated from the energy generation part during organic

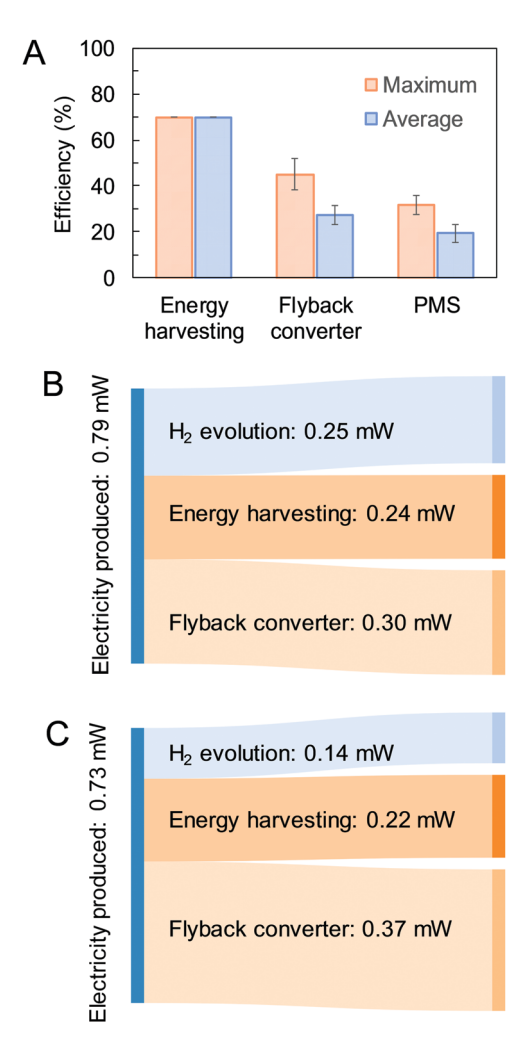


Fig. 4 Efficiency of the energy harvesting circuit, flyback converter and PMS (A), power flow of the spontaneous H₂ evolution system with maximum PMS efficiency (B) and average PMS efficiency (C).

degradation on the bioanode. This power was subsequently consumed by the energy harvesting circuit, the flyback converter, and the H₂ evolution reaction, respectively. Fig. 4A demonstrates that the energy harvesting circuit had an efficiency of 70% (a fixed value by the manufacturer's instruction), and the flyback converter had an efficiency of 45.1%, which resulted in a maximum efficiency of 31.6% of the PMS. However, due to the ripple in the current, the efficiency of the PMS fluctuated and averaged at 19.2% with a corresponding average flyback efficiency of 27.4% (Fig. 4A). The energy flow presented in Fig. 4B and C shows how much power each part of the system consumed to enable spontaneous H₂ generation from organic matter. In the case where the PMS showed the maximum efficiency, a highest power of 0.25 mW was achieved in the H₂ evolution reaction, representing 31.6% of the produced power from the energy generation part (Fig. 4B). The energy harvesting circuit consumed 0.24 mW to drive the magnification of the voltage. This circuit is a commercial circuit from Texas Instruments with a known power consumption.²⁷ The flyback converter required another 0.30 mW to operate, which occupied the greatest fraction,

38.0%, of the total produced power. The losses in the flyback converter were primarily in the transformer and diode, where the transformer incurred core and conduction losses as well as resistance in the windings, while the diode presented losses due to the threshold voltage and forward resistance. However, to compare with similar flyback converters designed for other low power energy systems, the >25% energy conversion efficiency was normal.²⁶ Fig. 4C shows the energy flow calculated using the average PMS efficiency. On average, 0.14 mW was used by the H₂ evolution reaction, representing 19.2% of the total generated power. Further considering the 91.3% H₂ generation efficiency on the cathode, the overall conversion efficiency could reach a maximum of 28.9% and an average of 17.5%.

Even though the efficiency could be improved, this proof-ofconcept study demonstrates that without this electrical decoupling the electrochemical reactions and temporary energy storage/ transfer would not be achieved, not to mention spontaneous H₂ evolution. This invention itself saved energy and presumably cost compared with previous studies that used external power sources to realize water splitting. The system efficiency can be further improved by improving the efficiencies of both the energy harvesting circuit and the flyback converter, using a bioanode to replace the OER anode to reduce the load of the PMS, and optimizing the configuration design to reduce the internal resistance.

Conclusions

This study demonstrates an electrical decoupling method that enabled spontaneous H2 production from organic waste treatment. The PMS decoupled bioanode organic oxidation from cathode proton reduction in the same electrolyte. The tailored PMS realized this decoupling by using an energy harvesting circuit to collect the energy generated from organic chemicals and magnified the voltage from 0.35 V to 2.2-2.5 V in situ, where the electromagnetic transformer transferred the energy and allowed water splitting without consuming any external energy. Without such a decoupling strategy, some types of external energy input such as an external power supply, another renewable energy system, or sunlight incidence are necessary to close the thermodynamic gap of water electrolysis. Thus, real self-sustaining wastewater-to-hydrogen spontaneous conversion was achieved. The system demonstrated good conversion efficiency, with a H₂ producing rate of 2.75 mL L⁻¹ day⁻¹, a cathode faradaic efficiency of 91.3%, and a maximum overall bioelectrochemical energy to H₂ conversion efficiency of 28.9%.

Experimental procedure

Power management system (PMS)

The tailored PMS was designed to have two major circuits (Fig. 2). One circuit was for energy harvesting, which collected the electricity generated from organic degradation and boosted the input voltage by >6 times as the output voltage. This integrated energy harvesting circuit utilized a PFM boost converter/charger (BQ25505, Texas Instruments Inc.) to boost the voltage from 0.35 V (the output voltage of the energy generation part) to ~ 2.2 V to power water electrolysis. The minimum voltage necessary to power the BQ25505 is 0.1 V per the manufacturer's instructions, and no external energy was needed for the operation of this circuit. The second circuit was a flyback converter (a transformer-based DC-DC converter), which was designed specifically for this study using the theory of pulse-width modulated DC-DC power converters by Marian K Kazimiercizuk.²⁹ The flyback converter built for this study (Fig. 2, the blue dotted box) comprises a transformer 78601/ 9MC from Murata Power Solutions (T), a fast switching diode Vishay 1N4448 (D), a capacitor 100 μF (C), and a MOSFET 3NL01C (S). The control was performed by an oscillator/timer TS3003 from Silicon Lab, delivering a pulse-width modulation of 9 kHz frequency and a duty cycle of 50%. This oscillator was powered by the 2.3 V output of the energy harvesting circuit, so no external energy was needed.

The magnetizing inductance of the transformer L_m played a critical role in the PMS energy storage because even if no current was flowing in the secondary windings of the transformer, current would flow through the primary windings on L_m (Fig. 2A), and that is how the PMS in this study was storing the magnetic energy. When the MOSFET (S) was ON and the diode (D) was OFF, the primary windings of the transformer were storing energy in Lm, while when the MOSFET (S) was OFF and the diode (D) was ON, energy was transferred from the primary to the secondary windings of the transformer and then passed to the capacitor (C). This cycle of energy storage and transfer at high frequency (9 kHz in the flyback converter and variable frequency for the energy harvesting circuit using a PFM) enabled spontaneous water splitting without any external energy.

System construction

The microbial electrochemical water electrolyzer contained three functional components, the energy generation part, the PMS (introduced in the previous section), and the H₂ evolution part (Fig. 1). All these components were assembled in a cubicshape reactor that had a 7 cm inner diameter and 5 cm depth (Perspex) (ESI,† Fig. S2). The energy generation part consisted of a bioanode that employed bacteria to degrade organics to generate electrons, and an abiotic Pt/C air cathode that conducted O2 reduction. The anode was made of a carbon brush (5 cm diameter and 5 cm length) to support biofilm growth and conduct electrons. The air cathode of 7 cm in diameter was made from one carbon base layer, four polytetrafluoroethylene diffusion layers and one catalyst layer (0.5 mg Pt per cm²).³⁰ The catalyst layer faced the electrolyte and the diffusion layer was in contact with the air. A Ag/AgCl reference electrode (RE-5B, BASi, IN, USA; +0.210 V versus standard hydrogen electrode, 25 °C) was used for electrical characterization measurements. The H2 evolution part included a platinum wire anode for O2 generation and a platinum microelectrode (MF-2005, BASi, IN, USA) for H₂ evolution. The O₂ generation electrode was placed adjacent to the aforementioned air cathode to allow O2 consumption. A piece of glass fiber was placed in between the O2 generation anode and the H2 evolution cathode to further

secure the separation of the produced H₂ from any remaining O2. The whole electrolyzer was sealed up tightly using screws, rubber gaskets and glue. An air bag was connected to the top of the reactor for gas collection.

System operation

Fig. 1B shows the system schematic and electrode connection. The external circuit of the bioanode was connected to the O₂ reduction cathode via the energy harvesting circuit in the PMS, while the external circuit of the water oxidation anode was connected to the H₂ evolution cathode via the flyback converter in the PMS. The bioanode was inoculated using anaerobic sludge obtained from a municipal wastewater treatment plant.³¹ The bioanode was grown in a microbial electrolysis cell using a nickel-foam cathode under an applied voltage of 0.8 V for 30 days before transferring to the experiment reactor.³² During the time of acclimation, the bioanode was enriched with an electroactive biofilm and could stably support a current around 10 mA. The bioanode could support a stable voltage output of 0.35 V and maintained a stable current output during multiple cycles of operation (ESI,† Fig. S1). The electrolyte utilized for conducting the experiments in this study contained (per liter): 1.64 g NaAc, 0.31 g NH₄Cl, 0.1 g CaCl₂, 0.1 g MgCl₂, and 100 mM phosphate buffer.³³ The reactor was operated in fed-batch mode with a cycle time of 96 h. The operation of the PMS was solely powered by the electricity generated from the system itself.

Analyses and calculations

The output voltage of the energy generation part and the voltage output of the PMS for H₂ evolution were recorded every 30 min using a data acquisition system (2700, Keithley Instruments, OH, USA).³⁴ The current (I) in both parts was calculated by I = U/R (mA), respectively, where U (mV) was the voltage across a 0.5 Ω resistance and R was 0.5 Ω . The power (P) was calculated from $P = UI \text{ (mW)}.^{35}$ The gases collected in the air bag were tested using a gas chromatograph (Model 8610C, SRI Instruments).19 The hydrogen volume was calculated by multiplying the total volume of the collected gas by the hydrogen content measured by a gas chromatograph. The chemical oxygen demand (COD), electrolyte conductivity, and pH were measured using standard methods.³²

Author contributions

X. C., F. L. L. and Z. J. R. wrote the manuscript. X. C. and F. L. L. conducted the experiment and characterization. Y. B. and L. L. assisted in reactor operation and analyses. X. W. C., M. T., and Y. W. assisted in circuit testing and energy related calculations.

Conflicts of interest

The authors declare no competing interests.

Acknowledgements

This work is supported by the US National Science Foundation under award CBET-1834724 and National Renewable Energy Laboratory under Contract No. XFF-8-82229-01. We thank Dianxun Hou for the help with H₂ measurement.

References

- 1 S. Chu and A. Majumdar, Nature, 2012, 488, 294.
- 2 Z. W. Seh, J. Kibsgaard, C. F. Dickens, I. Chorkendorff, J. K. Nørskov and T. F. Jaramillo, Science, 2017, 355, eaad4998.
- 3 J. A. Turner, Science, 2004, 305, 972.
- 4 A. G. Wallace and M. D. Symes, Joule, 2018, 2, 1390-1395.
- 5 Y. Goto, T. Hisatomi, Q. Wang, T. Higashi, K. Ishikiriyama, T. Maeda, Y. Sakata, S. Okunaka, H. Tokudome, M. Katayama, S. Akiyama, H. Nishiyama, Y. Inoue, T. Takewaki, T. Setoyama, T. Minegishi, T. Takata, T. Yamada and K. Domen, Joule, 2018, 2, 509-520.
- 6 V. Khare, S. Nema and P. Baredar, Renewable Sustainable Energy Rev., 2016, 58, 23-33.
- 7 L. Lu and Z. J. Ren, Bioresour. Technol., 2016, 215, 254-264.
- 8 J. A. Rollin, J. Martin del Campo, S. Myung, F. Sun, C. You, A. Bakovic, R. Castro, S. K. Chandrayan, C.-H. Wu, M. W. W. Adams, R. S. Senger and Y. H. P. Zhang, Proc. Natl. Acad. Sci. U. S. A., 2015, 112, 4964.
- 9 K. Zeng and D. Zhang, Prog. Energy Combust. Sci., 2010, 36, 307-326.
- 10 J. Rossmeisl, A. Logadottir and J. K. Nørskov, Chem. Phys., 2005, 319, 178-184.
- 11 S. Chen, Y. Qi, C. Li, K. Domen and F. Zhang, Joule, 2018, 2, 2260-2288.
- 12 B. Zhang and L. Sun, Chem. Soc. Rev., 2019, 48, 2216-2264.
- 13 B. E. Logan, D. Call, S. Cheng, H. V. M. Hamelers, T. H. J. A. Sleutels, A. W. Jeremiasse and R. A. Rozendal, Environ. Sci. Technol., 2008, 42, 8630-8640.
- 14 H. Liu, S. Grot and B. E. Logan, Environ. Sci. Technol., 2005, 39, 4317-4320.
- 15 A. J. Bard and M. A. Fox, Acc. Chem. Res., 1995, 28, 141-145.
- 16 N. S. Lewis, Nature, 2001, 414, 589.
- 17 M. G. Walter, E. L. Warren, J. R. McKone, S. W. Boettcher, Q. Mi, E. A. Santori and N. S. Lewis, Chem. Rev., 2010, 110, 6446-6473.
- 18 L. Lu, N. B. Williams, J. A. Turner, P.-C. Maness, J. Gu and Z. J. Ren, Environ. Sci. Technol., 2017, 51, 13494-13501.
- 19 L. Lu, W. Vakki, J. A. Aguiar, C. Xiao, K. Hurst, M. Fairchild, X. Chen, F. Yang, J. Gu and Z. J. Ren, Energy Environ. Sci., 2019, 12, 1088-1099.
- 20 D. Kong, X. Xie, Z. Lu, M. Ye, Z. Lu, J. Zhao, C. S. Criddle and Y. Cui, Nano Energy, 2017, 39, 499-505.
- 21 E. Suraniti, P. Merzeau, J. Roche, S. Gounel, A. G. Mark, P. Fischer, N. Mano and A. Kuhn, Nat. Commun., 2018,
- 22 M. D. Symes and L. Cronin, Nat. Chem., 2013, 5, 403.
- 23 B. Rausch, M. D. Symes, G. Chisholm and L. Cronin, Science, 2014, 345, 1326.

- 24 V. Amstutz, K. E. Toghill, F. Powlesland, H. Vrubel, C. Comninellis, X. Hu and H. H. Girault, Energy Environ. Sci., 2014, 7, 2350-2358.
- 25 A. Landman, H. Dotan, G. E. Shter, M. Wullenkord, A. Houaijia, A. Maljusch, G. S. Grader and A. Rothschild, Nat. Mater., 2017, 16, 646.
- 26 M. Alaraj, Z. J. Ren and J.-D. Park, J. Power Sources, 2014, 247, 636-642.
- 27 F. L. Lobo, X. Wang and Z. J. Ren, J. Power Sources, 2017, **356**, 356-364.
- 28 H. Wang, J.-D. Park and Z. J. Ren, Environ. Sci. Technol., 2015, 49, 3267-3277.
- 29 K. Kazimierczuk Marian and M. K. Kazimierczuk, Pulsewidth Modulated DC-DC Power Converters, Wiley, Dayton, Ohio, 2012.

- 30 S. Cheng, H. Liu and B. E. Logan, Environ. Sci. Technol., 2006, 40, 364-369.
- 31 D. Hou, A. Iddya, X. Chen, M. Wang, W. Zhang, Y. Ding, D. Jassby and Z. J. Ren, Environ. Sci. Technol., 2018, 52, 8930-8938.
- 32 X. Chen, R. Katahira, Z. Ge, L. Lu, D. Hou, D. J. Peterson, M. P. Tucker, X. Chen and Z. J. Ren, Green Chem., 2019, 21,
- 33 X. Chen, H. Sun, P. Liang, X. Zhang and X. Huang, J. Power Sources, 2016, 324, 79-85.
- 34 Y. Gao, D. Sun, H. Wang, L. Lu, H. Ma, L. Wang, Z. J. Ren, P. Liang, X. Zhang, X. Chen and X. Huang, Environ. Sci.: Water Res. Technol., 2018, 4, 1427-1438.
- 35 W. Wang, P. E. Jenkins and Z. Ren, Corros. Sci., 2012, 57,